0026-895X/94/061153-07$03.00/0

MOLECULAR PHARMACOLOGY, 45:1153-1159, 1994.

# Dual Regulation of Cytochrome P450EF Expression via the Aryl Hydrocarbon Receptor and Protein Stabilization in C3H/10T1/2 Cells

ÜZEN SAVAS and COLIN R. JEFCOATE

*Department of Pharmacology, University of Wisconsin Medical School, Madison, Wisconsin 53706*

Received June 14, 1993; Accepted March 22, 1994

**SUMMARY**

The major cytochrome P450 (P450EF) in the mouse embryo fibroblast C3H/10T1/2CL8 (10T1/2) cell line, which is very active in polycyclic aromatic hydrocarbon metabolism, is immunologically distinct from known P450 families but shares homology with an adrenocorticotropin hormone-regulated P450 from rat adrenal glands (P450RAP). P450EF is more effectively induced by benz[*a*]anthracene (BA) than by 2,3,7,8-tetrachlorodibenzo-*p*-dioxin (TCDD), which is anomalous for aryl hydrocarbon receptor (AhR)-mediated transcriptional activation. Evidence is presented here that induction of P450EF is consistent with mediation by the AhR but also involves an additional selective stabilization of P450EF by BA. P450EF-specific mRNA was measured by *in vitro* translation of 10T1/2 mRNA and subsequent immunoprecipitation with antibodies that recognize P450EF. P450EF mRNA was equally stimulated (>10-fold) by BA (10 μM) and TCDD (10 nM) after 6 hr of induction in 10T1/2 cells. This equal stimulation of P450EF by BA and TCDD is consistent with transcriptional activation of the gene by the AhR. BA induction of mRNA declined 3-fold between 6 and 18 hr, due to metabolism of BA. Steady state P450EF mRNA levels declined quickly once this stimulation was removed, whereas total P450EF protein levels, measured by immunoblotting, continued to increase. During a 6-hr inhibition of protein synthesis with cycloheximide, both total P450EF and functional cytochrome, measured by polycyclic aromatic hydrocarbon metabolism, decreased by 60% in uninduced and TCDD-induced transformed 10T1/2 cells. This is consistent with relatively rapid degradation of P450EF ($t_{½}$ = 4 hr). No such decline was seen when BA was present, indicating a stabilization of P450EF, which can explain the additional effectiveness of BA in enhancing the level of P450EF.

Increased P450 can be attributed to receptor-mediated transcriptional activation of the gene, post-transcriptional mRNA stabilization, or substrate-induced post-translational protein stabilization (1). Induction of P450s by PAHs, such as 3-methylcholanthrene or BA, or halogenated aromatic hydrocarbons, such as TCDD, is controlled by binding to the cytosolic AhR (2–4). Expression of both members of the *CYP1* gene family (*CYP1A1* and *CYP1A2*) is stimulated by PAH binding to the AhR. This produces enhanced rates of transcription of the activated gene in isolated hepatocytes and in liver of mice (5–7) and rats (8–10).

The action of the AhR in the induction of *CYP1A1* has been extensively studied in variants of Hepa-1 cells, and this has established the role of a functional TCDD-receptor complex in the expression of *CYP1A1* (11–14). The cytosolic receptor has been characterized as a helix-loop-helix protein (15, 16) that translocates into the nucleus after ligand binding and dissociation of the 90-kDa heat shock protein (17–19). The AhR binds, as a heterodimer with the AhR nuclear translocator protein (20), to multiple DNA recognition motifs (dioxin-responsive elements) upstream of exon 1 of *CYP1A1* to activate its transcription (21, 22).

CYP1A1 is the most active P450 in the metabolism of PAHs (23). The mouse embryo fibroblast 10T1/2 cell line converts a high proportion of PAHs to the carcinogenic dihydrodiol epoxides through a PAH-inducible reaction (24–26). However, *Cyp1a-1* gene expression in 10T1/2 cells after induction by TCDD and BA is extremely low (26), even though the AhR effectively stimulated a *Cyp1a-1* promoter-reporter fusion gene transiently transfected into 10T1/2 cells, thus indicating active AhR complexes (27). A novel PAH-metabolizing P450, temporarily denoted as P450EF, has been identified in these cells and is induced by both TCDD and BA (26). P450EF comprises

Ü.S. was partly supported by the Gottlieb Daimler and Karl Benz Foundation. This research was supported by National Institutes of Health Grant CA16265 and in part by Council for Tobacco Research USA, Inc., Grant 2963.

**ABBREVIATIONS:** P450, cytochrome P450; PAH, polycyclic aromatic hydrocarbon; BA, benz[*a*]anthracene; TCDD, 2,3,7,8-tetrachlorodibenzo-*p*-dioxin; AhR, aryl hydrocarbon receptor; DMBA, 7,12-dimethylbenz[*a*]anthracene; DMSO, dimethylsulfoxide; 10T1/2, C3H/10T1/2CL8; MCA cells, 3-methylcholanthrene-transformed C3H/10T1/2CL8 cells; Hepa-1, Hepa-1c1c7; HPLC, high pressure liquid chromatography; SDS, sodium dodecyl sulfate; PAGE, polyacrylamide gel electrophoresis; TCA, trichloroacetic acid; PBS, phosphate-buffered saline.

the majority of the P450 content in 10T1/2 microsomes, both constitutively and after PAH induction. Purification and immunological characterization of this enzyme established the presence of a 55-kDa protein that is substantially distinct from CYP1A1, not only in terms of positional selectivity for DMBA metabolism but also in terms of immunological characteristics (26, 28). The use of specific antibodies established that essentially all PAH metabolism in 10T1/2 microsomes is catalyzed by this form (28). P450EF failed to cross-react with antibodies to members of the major microsomal families 1–4. However, P450EF exhibited cross-reactivity with an antibody to an adrenocorticotropin hormone-stimulated P450 isolated from rat adrenal cortex (P450RAP), which also showed similar PAH metabolic activity and regioselectivity (28–30). Studies from our laboratory showed that P450EF or the characteristic PAH metabolism is also expressed in stromal fibroblasts from rodent uterus (31), prostate (25), mammary gland,[1] and embryonic primary cultures.[2] Expression of P450EF in these endocrine tissues is induced by TCDD or PAH, suggesting the involvement of the AhR in the regulation of its expression.

Surprisingly, the maximum increase of functional P450EF in 10T1/2 cells produced by BA is 2 times greater than that produced by TCDD. This is unlike the normal regulation of expression via the AhR, where TCDD is typically the most effective ligand. In this report, we present an analysis of the regulation of P450EF by BA and TCDD at both the protein and mRNA levels. By utilizing a reticulocyte translation system to generate [$^{35}$S]apo-P450EF in proportion to the specific mRNA, we establish that maximum induction of P450EF mRNA is consistent with involvement of the AhR. In addition, we provide evidence for substrate-induced stabilization of P450EF protein by BA, which can account for the exceptional effectiveness of BA at the protein level.

## Experimental Procedures

**Chemicals.** DMSO, BA, and DMBA were purchased from Aldrich Chemical Co. (Milwaukee, WI). TCDD was obtained from Chemsyn Science Lab. (Lenexa, KS). L-[$^{35}$S]Methionine (1000 Ci/mmol) was purchased from Amersham (Arlington Heights, IL). The rabbit reticulocyte lysate, the ribonuclease inhibitor (RNasin), and the amino acid mixture (minus methionine) were purchased from Promega (Madison, WI). The fluorographic reagent Amplify was purchased from Amersham. The substrates for the color development, i.e., nitroblue tetrazolium and 5-bromo-4-chloro-3-indolyl phosphate, were obtained from Promega. Oligo(dT)-cellulose (type 3) was purchased from Collaborative Research, Inc. (Bedford, MA). Coomassie brilliant blue, gentamicin sulfate, and cycloheximide were obtained from Sigma Chemical Co. (St. Louis, MO). Bicinchoninic acid assay reagents were purchased from Pierce Chemcial Co. (Rockford, IL). Pansorbin was obtained from Calbiochem. (La Jolla, CA) and Nonidet P-40 from Particle Data Lab. (Elmhurst, IL).

**Antibodies.** Polyclonal anti-P450EF (28), anti-P450RAP (29), and anti-CYP1A1 (26) served as primary antibodies for the Western immunoblots and the immunoprecipitations. Anti-$\beta$-actin serum was purchased from Sigma Immunochemicals (St. Louis, MO). Goat anti-rabbit IgG-alkaline phosphatase conjugate was obtained from Promega.

**Cell culture and treatments.** 10T1/2, MCA, and Hepa-1 cells were grown in Dulbecco's modified Eagle's medium (GIBCO) supplemented with 10% fetal bovine serum (Gemini) and gentamicin sulfate. 10T1/2 and Hepa-1 cells were treated at 80% confluence with either 0.1% DMSO, 10 $\mu$M BA, or 10 nM TCDD. MCA cells were grown in Dulbecco's modified Eagle's medium/F-12 medium (1:1; GIBCO) supplemented with 10% fetal bovine serum and gentamicin sulfate. At 8 days after confluence, cells were treated, as a multilayer culture, with the respective inducer. Between 18 and 24 hr of exposure to the inducer, cycloheximide treatments were performed at a final concentration of 10 $\mu$M. DMSO-treated cells (uninduced) were exposed to cycloheximide for a period of 6 hr.

**Preparation of microsomes and metabolism assay.** Cells were harvested after 6, 18, and 24 hr of treatment, washed in ice-cold PBS, and stored in liquid nitrogen. Microsomes from all groups of treatments were prepared as described previously (26). The protein concentrations were assayed by the bicinchoninic acid method. The DMBA-metabolizing profiles of P450EF were determined according to previously described methods (32). Microsomal incubations were carried out at 0.5 mg/ml. After a 5-min preincubation at 37°, reactions were initiated by addition of 10 $\mu$M DMBA. Reactions were stopped after 15 min of DMBA metabolism, and metabolites were extracted and prepared for analysis by HPLC according to previously described methods (32).

**Electrophoresis and Western immunoblotting.** Microsomal proteins were separated by SDS-PAGE (7.5% acrylamide) according to the method of Laemmli (33) and were transferred to nitrocellulose. Cross-reactive proteins were visualized with goat anti-rabbit IgG coupled to alkaline phosphatase, using nitroblue tetrazolium and 5-bromo-4-chloro-3-indolyl phosphate as substrates for the color reaction (26). The induction factor of P450EF relative to constitutive levels was determined by comparing densitometric scans of immunoblots obtained at several microsomal loadings and by averaging the integration ratios from five independent microsomal preparations.

**Total RNA isolation.** The isolation of total RNA from cultured cells and selection of poly(A)$^+$ mRNA were performed according to standard protocols, using the guanidinium isothiocyanate method and two cycles with oligo(dT), at an oligo(dT)/RNA ratio of 0.1 g/400 $\mu$g (34).

***In vitro* translation and subsequent immunoprecipitation.** Total RNA or mRNA was translated (1 hr at 30°) in a rabbit reticulocyte translation system (minus methionine) using 40 $\mu$Ci of [$^{35}$S] methionine as a radiolabel, with 1 unit of RNasin, according to the protocol of Promega. Varying amounts of 10T1/2 mRNA were used to establish an approximately linear relationship between the amount of translated mRNA and [$^{35}$S]methionine incorporated into newly synthesized protein. Thus, 2, 4, 5, and 6 $\mu$g of mRNA, when incubated in the rabbit reticulocyte translation system, provided the following amounts of $^{35}$S-protein: 1.1, 2.3, 2.9, and 5.5 $\times$ 10$^4$ cpm/$\mu$l of translation product, respectively. Five micrograms of mRNA were used for each subsequent *in vitro* translation.

In detail, the method for quantitation of [$^{35}$S]P450EF was as follows. Aliquots of reticulocyte translation product (2 $\times$ 2 $\mu$l) were removed to determine the total incorporation of [$^{35}$S]methionine into newly synthesized proteins. Translation product (2 $\mu$l) was incubated with 1 N NaOH/2% $H_2O_2$ (123 $\mu$l) for 10 min at 37°, mixed with ice-cold 25% TCA (0.5 ml) and 5% bovine serum albumin (10 $\mu$l), and incubated for 10 min on ice. TCA precipitates were recovered by centrifugation (30 sec, 13,000 $\times$ $g$), dissolved in 0.4 ml of 0.1 N KOH, and reprecipitated with 0.5 ml of 25% TCA. Pellets were dissolved in 0.5 N KOH and transferred for radioactivity counting. These measurements were used to submit the same amount of $^{35}$S-translation product for immunoprecipitation, by adjustment of the amount withdrawn.

Immunoprecipitation was carried out by sequestering specific antibody complexes to Pansorbin according to previously described methods (35, 36). Equal levels of $^{35}$S-translation product from each reaction (1.3 $\times$ 10$^6$ cpm) were mixed with an equal volume of 10% SDS solution, and then samples were boiled (3 min) and diluted 10-fold in PBS, pH 7.0, supplemented with 1 mM EDTA, pH 8.0, and 0.5% Nonidet P-40. To remove proteins that bind nonspecifically, Pansorbin (40 $\mu$l) that had been prewashed with PBS containing 1 mM EDTA and 0.25% Nonidet P-40 was first incubated with each sample for 1 hr at room

[1] M. Christou, Ü. Savas, and C. R. Jefcoate, unpublished observations.
[2] D. L. Alexander and C. R. Jefcoate, unpublished observations.

temperature. After centrifugation (10 min at 130,000 × g), supernatants were incubated with 20 μg of preimmune IgG at room temperature for 20 min and then with Pansorbin (40 μl) for another 1 hr. After an additional centrifugation, supernatants were incubated with 12 μg of specific immune IgG (anti-P450RAP, anti-CYP1A1, or anti-β-actin) at 4° overnight and then with Pansorbin (40 μl) for another 10 min at room temperature. After centrifugation, pellets containing Pansorbin-bound IgG-protein complex were suspended in PBS (300 μl) supplemented with 1 mM EDTA, 0.5% Nonidet P-40, 0.1% SDS, and 10 mM methionine and were centrifuged through 1.5 M sucrose (1 ml). Pellets were then repeatedly washed in this buffer until radioactivity reached constant levels. Pellets were resuspended in Laemmli electrophoresis buffer and boiled for 3 min; 10% of the supernatant was used to measure the total radioactivity of the immunoprecipitate and 90% was applied for SDS-PAGE.

**Analysis of immunoprecipitated protein.** Total immunoprecipitates were analyzed by SDS-PAGE (7.5% or 12% acrylamide). After electrophoretic separation of proteins, gels were fixed in isopropanol/water/acetic acid (25:65:10, 30 min) and soaked in Amplify for fluorography (30 min). Gels were dried (2 hr at 60°) and exposed to Kodak X-ray film; exposure times ranged between 1 and 60 days. Pure rat hepatic CYP1A1 (1 μg) was added as a standard on every gel containing the immunoprecipitates and was stained separately with Coomassie brilliant blue. The relative mobility of CYP1A1 was used as a molecular weight marker for the immunoprecipitated protein.

## Results

**Quantitation of P450EF protein levels in 10T1/2 and MCA cells.** Immunoblots with anti-P450EF were used to quantitate levels of P450EF in both 10T1/2 and MCA cell lines (Fig. 1A). These immunoblots measured total P450EF in the microsomes (subsequently referred to simply as total P450EF), which comprised functional hemoprotein and potentially a proportion of apoprotein. Based on these immunoblots, total P450EF was present at comparable levels in microsomes from untreated 10T1/2 and MCA cells. In both cell lines, basal expression of total P450EF was stimulated to a greater extent by BA than by TCDD. Densitometric analysis of immunoblots from three 10T1/2 and five MCA cell microsomal preparations showed an average total P450EF induction factor of 17 ± 2.1 for BA and 6 ± 1.2 for TCDD. BA was therefore 3-fold more effective than TCDD in elevating total P450EF in both cell lines, whereas CYP1A1 was undetectable after treatment with either BA or TCDD (Fig. 1B).

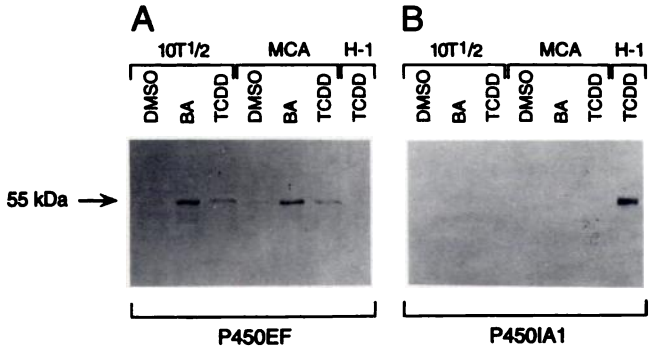


**Fig. 1.** Induction of total P450EF in 10T1/2 and MCA cells. Microsomes from DMSO-, BA-, and TCDD-treated 10T1/2 and MCA cells, as well as microsomes from TCDD-treated Hepa-1 cells, were prepared after 24 hr of induction. Microsomal proteins (8 μg/lane) were separated by SDS-PAGE and transferred to nitrocellulose. Visualization of immunoreactive proteins was achieved by the alkaline phosphatase method. A, Immunoblot with anti-P450EF; B, immunoblot with anti-P450IA1 (CYP1A1).

Functional P450EF, measured by total DMBA-metabolizing activity, was induced similarly in both 10T1/2 and MCA cell lines. The average induction factor for this activity, determined from three independent experiments, was 8.0 ± 1.1 for BA and 5.0 ± 0.9 for TCDD. Surprisingly, for both 10T1/2 and MCA cells the ratio of BA/TCDD induction was always higher for total P450EF levels measured by immunoblots (3.3 ± 0.6) than for functional P450EF measured by DMBA metabolism (1.7 ± 0.2). This suggests that, when BA is the inducer, a significant proportion of the total P450EF is not optimally active in DMBA metabolism.

**Quantitation of P450EF mRNA levels.** P450EF mRNA was quantitated by immunoprecipitaion of [$^{35}$S]P450EF generated from *in vitro* reticulocyte translation of 10T1/2 mRNA. Anti-P450RAP, which immunoprecipitates P450EF more efficiently than does anti-P450EF, was used to immunoprecipitate [$^{35}$S]P450EF. The steady state level of P450EF mRNA was reflected by a 55-kDa immunoprecipitated protein (Fig. 2A). P450EF mRNA, measured from two independent immunoprecipitations, was increased 3-fold by BA and 6-fold by TCDD (Fig. 2B), reversing the effectiveness of the inducers at the protein level. There was no immunoprecipitable protein corre-

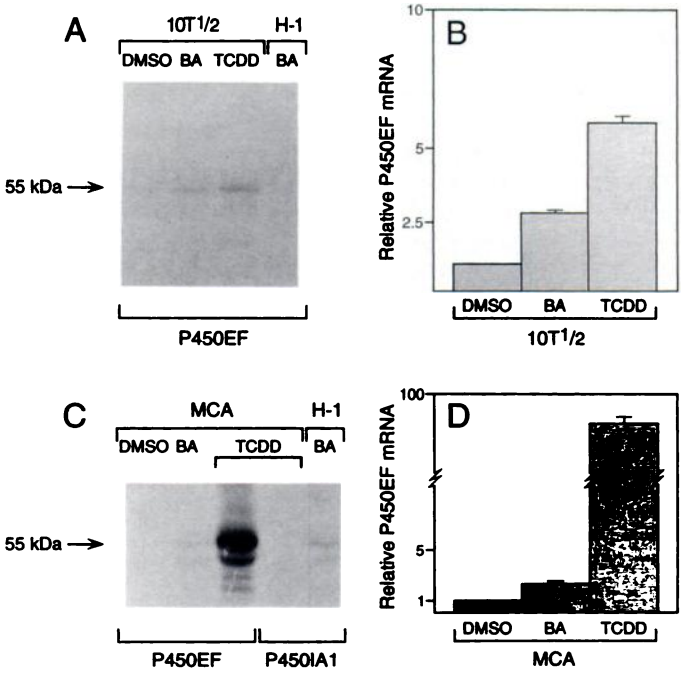


**Fig. 2.** Induction of P450EF mRNA levels in 10T1/2 and MCA cells. mRNA (5 μg) from DMSO-, BA-, and TCDD-treated 10T1/2 cells and from BA-treated Hepa-1 cells (24 hr) was translated in a rabbit reticulocyte translation system. Equal amounts of radioactivity (1.3 × 10$^6$ cpm) were utilized for each immunoisolation of P450EF with anti-P450RAP (12 μg). A, SDS-PAGE analysis of the immunoprecipitates after fluorography and autoradiography (10-day exposure). B, Relative inducibility of P450EF mRNA in 10T1/2 cells, derived from densitometric scans of the autoradiograms averaged for two independent experiments. *Error bars*, range of induction in these two experiments. C, Equivalent P450EF mRNA levels in MCA cells measured by reticulocyte translation, as described for A. CYP1A1 mRNA levels in TCDD-induced MCA cells and BA-induced Hepa-1 cells were compared by using anti-P450IA1 (CYP1A1). D, Inducibility of P450EF mRNA in MCA cells, derived from densitometric scans of autoradiograms averaged for three independent immunoprecipitations, showing the range of variability of induction from three experiments (*error bars*).

sponding to P450EF mRNA from BA-treated Hepa-1 cells (Fig. 2A).

The equivalent experiment with MCA cells (Fig. 2C) shows much larger differences in P450EF mRNA between the inducers. There was only a 3-fold increase of mRNA by BA, compared with >60-fold stimulation by TCDD (Fig. 2D). CYP1A1 was undetectable by this method in TCDD-induced MCA cells, consistent with previous CYP1A1 cDNA hybridization (37), whereas it was clearly detected in BA-induced Hepa-1 mRNA (Fig. 2C). A second, weaker, more mobile band was co-precipitated in each case at about one third the intensity of P450EF and was not identified. Immunoprecipitation of $\beta$-[$^{35}$S]actin from these mRNA translates as an internal standard (detected as a 45-kDa protein) indicated similar efficiency levels for each sample (data not shown).

**Time course for P450EF induction.** One possible explanation for the greatly diminished levels of BA-induced P450EF mRNA, relative to levels after TCDD treatment, in MCA cells is that BA is removed by metabolism in the 24-hr period before isolation of mRNA. To test this possibility, we measured P450EF mRNA steady state levels after 6 and 18 hr of induction with BA and TCDD. Two independent experiments showed that P450EF mRNA was equally induced by both inducers after 6 hr of treatment. After 18 hr, the TCDD induction level was maintained at the 6-hr level, whereas the BA induction level decreased 3-fold (Fig. 3, A and C). The corresponding total P450EF increased between 6 and 18 hr for both inducers, with greater effectiveness of BA (Fig. 3B). There was a 3-fold decline in BA-induced P450EF mRNA between 6 and 18 hr, concomitant with a 5-fold increase in the protein (Fig. 3D). DMBA metabolism provides a measure of functional P450EF, distinct from total protein. This activity also increased in parallel with total P450EF protein levels between 6 and 18 hr and showed a 2-fold decline after 24 hr of treatment with BA (Fig. 4A). The microsomal level of BA in MCA cells, which should be proportional to the residual cell BA, declined to <10% of initial levels after 18 hr and was almost undetectable at 24 hr (<0.5 pmol/mg of protein) (Fig. 4B). The capacity to deplete BA from the medium is proportional to cell density and is therefore higher for MCA cells, which, unlike 10T1/2 cells, grow as multilayers. Microsomal BA levels in high-density MCA cells at 18 hr were generally 5-fold lower than those in typical 10T1/2 induction experiments at 24 hr (Fig. 1).

Fig. 4C presents time courses for induction of DMBA metabolism by BA and TCDD in MCA cells at a lower cell density, comparable to that in 10T1/2 cells (Fig. 1). There was no decline of total DMBA-metabolizing activity between 18 and 24 hr of induction, consistent with slower removal of BA. TCDD- and BA-induced DMBA metabolism was equally stimulated after 6 hr, but BA was twice as effective during the next 12 hr. A similar late effect of BA was seen for total P450EF (Fig. 3D), except that differences between the inducers were larger.

**Turnover of P450EF.** The rapid decline of P450EF-dependent DMBA metabolism after depletion of BA suggested that the enzyme might be relatively labile in the absence of a substrate. To test this possibility, we examined the effect on P450EF levels of inhibiting new protein synthesis for a short period, thus providing a measure of the removal rate. The same period of inhibition was examined in uninduced cells and in cells maintained with either TCDD or an excess of BA (boosted

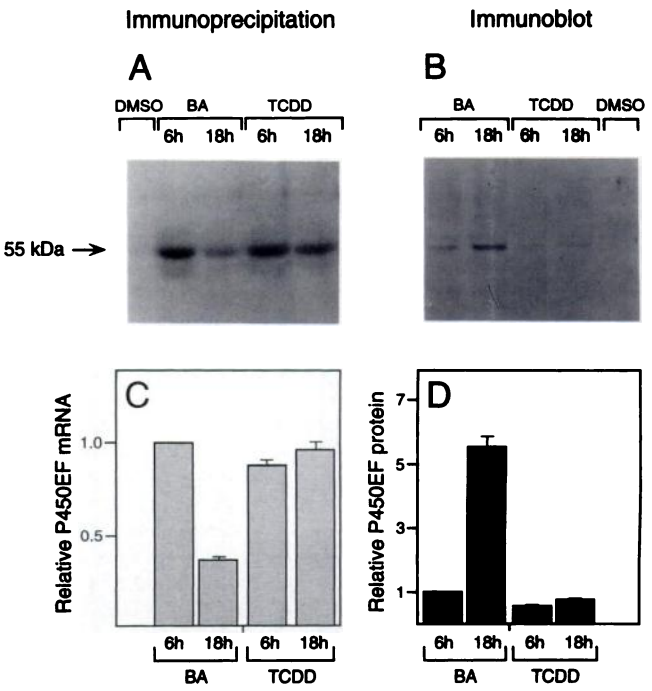


**Fig. 3.** Time dependence of P450EF mRNA and total protein induction in MCA cells. P450EF mRNA levels quantitated by reticulocyte translation and immunoprecipitation are compared with the corresponding microsomal P450EF protein levels quantitated by immunoblots. A, SDS-PAGE analysis of immunoprecipitations from translated mRNA isolated from DMSO-, BA-, or TCDD-induced MCA cells (treated for 6 or 18 hr). Equal amounts of radioactivity ($1.5 \times 10^6$ cpm) were utilized to immunoprecipitate P450EF with anti-P450RAP. B, Immunoblots of the corresponding P450EF from microsomal preparations. Microsomal proteins (8 $\mu$g/lane) were separated by SDS-PAGE and transferred to nitrocellulose. Visualization of immunoreactive proteins was accomplished by using the alkaline phosphatase method. C and D, Relative P450EF mRNA (C) and total P450EF (D) levels averaged from densitometric scans of the autoradiograms and the immunoblots obtained from two independent experiments. *Error bars*, range of variability of induction in these two experiments.

at 12 hr of induction). Inhibition of protein synthesis was achieved with cycloheximide treatment, which was applied for a period of 6 hr, beginning at a time when maximum induction had been achieved (after 18 hr). When cells were treated with BA, total P450EF (Fig. 5A) and DMBA-metabolizing activity (Fig. 4C) increased slightly from 18 to 24 hr and were largely insensitive to the 6-hr cycloheximide treatment (Figs. 5A and 6). In contrast, microsomes from TCDD-induced cells exhibited a 2–5-fold decline in DMBA metabolism (Fig. 6) and a 5-fold decline in TCDD-induced total P450EF (Fig. 5A) when protein synthesis was inhibited. The same period of protein synthesis inhibition in uninduced cells produced almost the same effect as in TCDD-induced cells; there was a 5-fold decrease of constitutive total P450EF (Fig. 5B) and a 3-fold decline in DMBA metabolism (Fig. 6).

Efforts have been made to measure the turnover of P450EF and the post-translational regulation of BA more directly, by pulse-chase labeling of uninduced, BA-induced, and TCDD-induced MCA cells. Attempts were made to assess P450EF levels from specific immunoprecipitations after 2 hr of [$^{35}$S] methionine labeling (35). Unfortunately, we could not detect an inducible 55-kDa $^{35}$S-labeled protein that would correspond to the less abundant P450EF, whereas simultaneously conducted immunoprecipitations of $\beta$-actin revealed a 45-kDa pro-

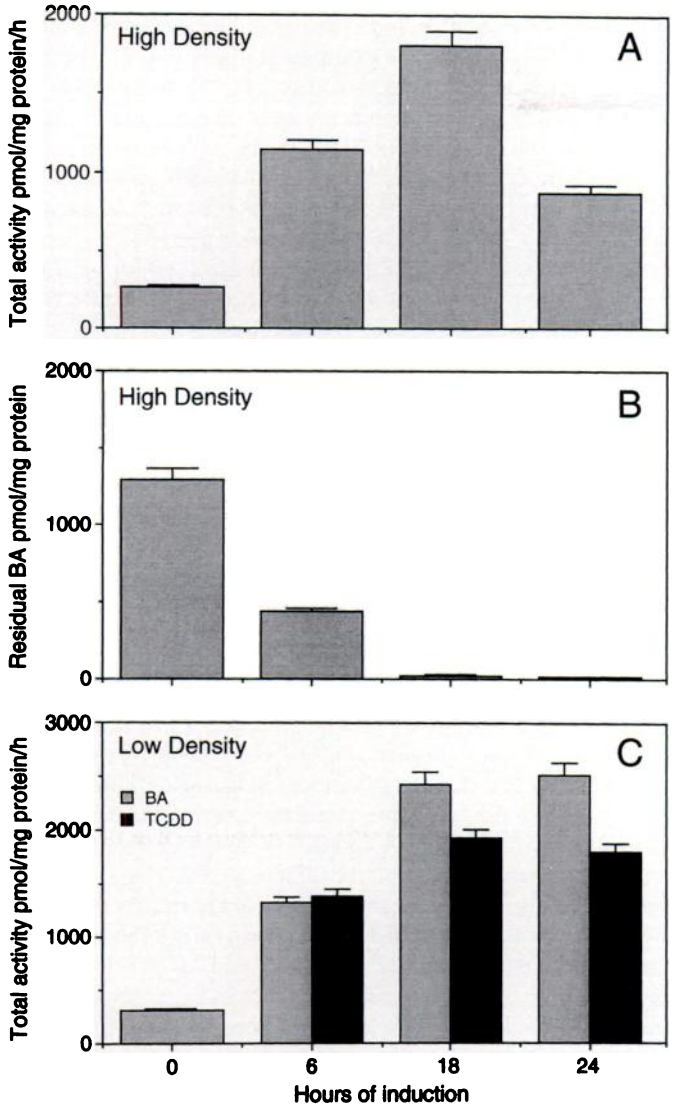


**Fig. 4.** Time course of functional P450EF induction in MCA cells. Total DMBA metabolism was measured with BA-treated (10 μM) MCA cell microsomes prepared after 6, 18, or 24 hr of induction or 24 hr of DMSO treatment (0 hr of induction). A, Conditions of high density of MCA cells and a single treatment with BA. Data shown represent total DMBA metabolism averaged from two separate microsomal incubations. B, Corresponding residual microsomal BA levels in the cells, determined by HPLC analyses. C, Total DMBA-metabolizing activity from MCA cell microsomes prepared after 6, 18, or 24 hr of either BA (10 μM) or TCDD (10 nM) treatment. The BA concentration was boosted with an additional 10 μM BA at 12 hr of induction, to ensure the presence of the inducer throughout the induction time. Data show the average total DMBA-metabolizing activity from two separate microsomal incubations. *Error bars*, variability within these incubations.

tein that was clearly distinguishable against the background. Immunoprecipitation from cell lysates seems to provide less efficient immunoprecipitation than seen with the reticulocyte translation system, possibly because of unusually strong binding of this type of P450 to membrane phospholipids, as has been observed during purifications of P450EF and P450RAP (28, 29).

## Discussion

The induction by PAH and TCDD of P450EF in 10T1/2 cells suggests that the AhR mediates this process in much the same way as has been established for CYP1A1 induction (3, 6, 38). The $EC_{50}$ for induction by TCDD of P450EF-mediated metabolism in 10T1/2 cells (about 0.1 nM) is fully consistent with this mechanism.[3] However, BA, a relatively weak AhR agonist, is 2–3 times more effective in elevating levels of P450EF in 10T1/2 cells than is TCDD, the strongest agonist (2, 3, 39), whereas the reverse is seen for the AhR-mediated induction of CYP1A1 in mouse Hepa-1 cells (26). Two sets of experiments presented in this paper establish a mechanism for P450EF induction that is consistent with mediation by the AhR but also explains the exceptional effectiveness of BA. We show that TCDD and BA are equally effective in elevating P450EF mRNA and that stimulation by BA declines as the inducer is metabolized, just as has been reported for induction of CYP1A1 in hepatocytes (40). The exceptional stimulation of

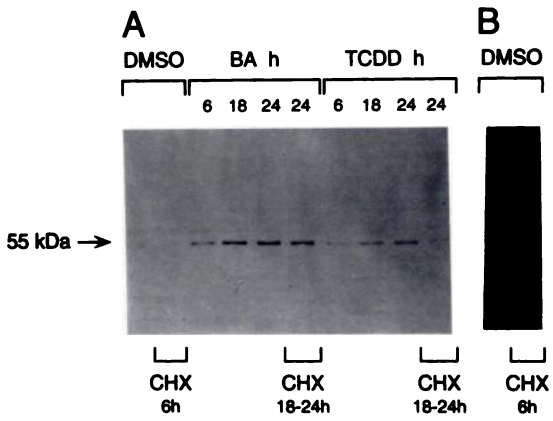


**Fig. 5.** Loss of total P450EF in MCA cells during cycloheximide (*CHX*) inhibition of protein synthesis. Microsomes were isolated after 6, 18, or 24 hr of BA or TCDD treatment or 24 hr of DMSO treatment. The indicated cycloheximide treatment was applied between 18 and 24 hr of induction. A, Immunoblot (with anti-P450EF) of microsomes (8 μg/lane) from DMSO-, BA-, and TCDD-treated cells and from cells that were simultaneously treated with cycloheximide for the final 6 hr. The BA concentration was boosted with an additional 10 μM BA at 12 hr of induction. B, Effect of cycloheximide on constitutive levels of P450EF measured at higher microsomal protein levels (15 μg/lane).

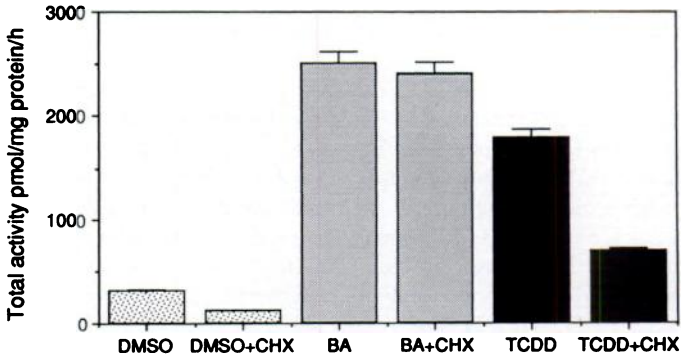


**Fig. 6.** Loss of DMBA functional P450EF in MCA cells during cycloheximide (*CHX*) inhibition of protein synthesis. The same microsomes described for Fig. 5, to which cycloheximide was added at a 10 μM final concentration between 18 and 24 hr of BA or TCDD induction, were analyzed for DMBA metabolism. Total activity of DMBA metabolism was determined after HPLC analysis of DMBA metabolites generated from microsomes prepared from 24-hr-treated cells. Data shown represent total DMBA metabolism from two separate microsomal incubations. *Error bars*, variability within two separate microsomal incubations.

[3] D. L. Alexander and C. R. Jefcoate, unpublished observations.

P450EF by BA arises because even very low concentrations of BA apparently slow the degradation of what is otherwise a very labile protein. The same regulation of P450EF is seen in both 10T1/2 and transformed MCA cells.

Steady state levels of P450EF mRNA in MCA and 10T1/2 cells have been quantitated by *in vitro* translation of mRNA, followed by immunoprecipitation with antibodies that specifically recognize P450EF. These antibodies immunoprecipitate a protein from reticulocyte-translated 10T1/2 mRNA with the same mobility (55 kDa) as P450EF in SDS-PAGE. Several additional experiments validate this approach. There was no immunoprecipitable protein translated from BA-induced Hepa-1 mRNA, which does not produce P450EF (26), whereas CYP1A1 was immunoprecipitable by anti-CYP1A1. In addition, only the related rat adrenal P450RAP (based on molecular weight and adrenocorticotropin hormone inducibility) (29) was immunoprecipitated by the same antibody from reticulocyte translates of rat adrenal cell mRNA (data not shown). Using this method, we showed that BA and TCDD produce similar maximum steady state levels of P450EF mRNA in both cell lines after 6 hr of treatment, whereas BA was relatively less effective at 18–24 hr as a result of metabolic depletion. This difference was even greater in MCA cells, which are not contact inhibited and consequently can grow to higher cell densities than 10T1/2 cells, resulting in much higher rates of BA depletion.

The time courses for BA stimulation of total P450EF and functional protein were very different from those for changes in mRNA. Both total P450EF protein and DMBA metabolism increased between 6 and 18 hr, indicating that loss of P450EF mRNA during this time is not paralleled by a loss of P450EF. This is very similar to previously reported differences in turnover of CYP1A1 mRNA and protein during treatments of rat hepatocytes (40), mouse liver, and extrahepatic tissues (38) with PAH. This difference in the time course for P450EF mRNA and protein can in part be attributed to unstable P450EF mRNA, which declines rapidly once the BA-activated transcription of P450EF mRNA slows, concomitant with depletion of BA. This, however, does not explain how protein continues to rise during removal of this inducer, while the mRNA level declines.

The substantial losses of total P450EF protein and activity that occurred when protein synthesis was briefly inhibited by cycloheximide indicate rapid turnover of the protein. In uninduced and TCDD-induced MCA cells, the approximately 4-fold loss of total P450EF and DMBA metabolism during the 6-hr period of inhibited protein synthesis is compatible with half-lives for hemoprotein and apoprotein of 3–4 hr. This may actually represent an underestimate of the degradation rate. The lesser utilization of amino acids for synthesis during cycloheximide treatment can cause a compensatory decrease in general protein degradation as this process becomes less necessary to replenish the amino acid pool (41). However, when BA was present in these cells, this cycloheximide treatment produced no discernible loss of P450EF, suggesting a half-life for P450EF of at least 24 hr. This decrease in degradation rate would be sufficient to cause a 5–10-fold elevation of P450EF without any increase in the rate of synthesis. Stabilization of P450EF through binding of BA in the substrate site is the simplest explanation for this slower degradation and would be analogous to substrate effects on other P450s (40, 42, 43). However, we cannot exclude the possibility of indirect effects of BA on this stability. For example, stability of CYP2 proteins can be decreased by phosphorylation (44). Cycloheximide may have additional effects within the cells. For example, superinduction caused by a cycloheximide-mediated increase of mRNA synthesis in TCDD-induced Hepa-1 cells has been reported for CYP1A1 catalytic activity (45). However, such changes in mRNA cannot contribute to the changes reported here, because translation was fully inhibited. An indirect effect of BA on P450EF through an additional labile protein that affects the turnover remains possible but seems unlikely.

BA produces a much larger increase in total P450EF than in the associated PAH metabolism, whereas for TCDD these changes are closely matched. This discrepancy could arise from 50% inhibition by a residual BA metabolite or an additional proportion of P450 apoprotein after BA induction (about 50%). The latter could readily arise if heme synthesis is limiting in these cells. Fig. 7 shows a general scheme for regulation of P450EF in 10T1/2 cells that incorporates processes of regulation described in this paper.

When administered together, TCDD and BA produce only a slightly greater enhancement of DMBA activity than does BA alone. This is consistent with BA exhibiting nearly maximal effectiveness at the AhR, which is not improved by the presence of TCDD. At low concentrations of BA it may be possible to see additivity between the two inducers, because BA apparently stabilizes P450EF at concentrations lower than those that stimulate synthesis. These conditions, however, would be difficult to control because of continuously changing concentrations of BA caused by metabolism. We are currently testing for PAHs that stabilize P450EF without activating the AhR. The natural turnover of P450EF in 10T1/2 and MCA cells is much more rapid than that reported for P450s in hepatocytes (11 hr) (40). This rapid turnover suggests an important role of P450EF in the regulation of key functions in these cells.

Recent work from this laboratory has described the isolation of a cDNA encoding P450EF from 10T1/2 cells. RNA hybridization of this cDNA revealed an mRNA species of 5.2 kilobases, which is 3 times longer than needed to encode the protein. The deduced amino acid sequence from this cDNA

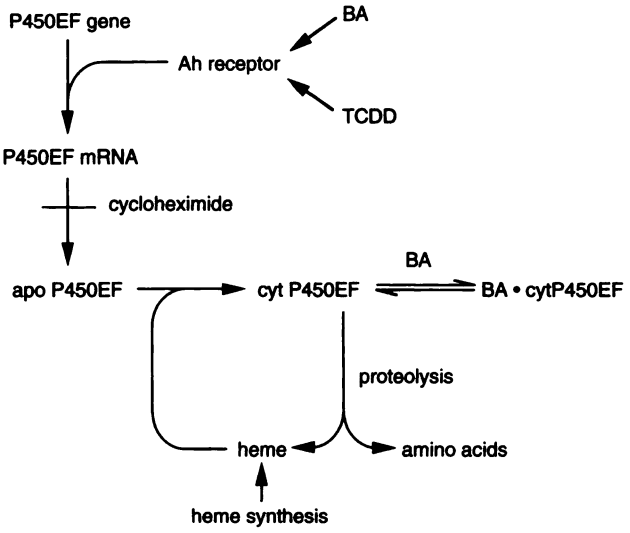


**Fig. 7.** Model for the regulation of P450EF turnover by BA and TCDD.

showed 41% similarity to the sequence of CYP1A1; consequently, P450EF has been designated CYP1B1 (46).

**Acknowledgments**

We wish to thank Dr. Mary E. Elliott for providing us with her *in vitro* translation and immunoprecipitation protocol and for many helpful discussions regarding these studies. We are grateful to Karen Wipperfurth and Teresa Schiffer for the preparation and final editing of the manuscript.

**References**

1. Porter, T. D., and M. J. Coon. Cytochrome P450. *J. Biol. Chem.* **266**:13469–13472 (1991).
2. Nebert, D. W., and F. J. Gonzalez. P450 genes: structure, evolution, and regulation. *Annu. Rev. Biochem.* **56**:945–993 (1987).
3. Whitlock, J. P., Jr. Genetic and molecular aspects of 2,3,7,8-tetrachlorodibenzo-*p*-dioxin action. *Annu. Rev. Pharmacol. Toxicol.* **30**:251–277 (1990).
4. Gonzalez, F. J. The molecular biology of cytochrome P450s. *Pharmacol. Rev.* **40**:243–288 (1989).
5. Miller, A. G., and J. P. Whitlock, Jr. Novel variants in benzo(*a*)pyrene metabolism. *J. Biol. Chem.* **265**:2433–2437 (1981).
6. Israel, D., and J. P. Whitlock, Jr. Regulation of cytochrome $P_1$-450 gene transcription by 2,3,7,8-tetrachlorodibenzo-*p*-dioxin in wild-type and variant mouse hepatoma cells. *J. Biol. Chem.* **259**:5400–5402 (1984).
7. Gonzalez, F. J., R. H. Tukey, and D. W. Nebert. Structural gene products of the *Ah* locus: transcriptional regulation of cytochrome $P_1$-450 and $P_3$-450 mRNA levels by 3-methylcholanthrene. *Mol. Pharmacol.* **26**:117–121 (1984).
8. Silver, G., and K. S. Krauter. Expression of cytochromes P-450c and P-450d mRNAs in cultured rat hepatocytes. *J. Biol. Chem.* **263**:11802–11807 (1988).
9. Silver, G., L. M. Reid, and K. S. Krauter. Dexamethasone-mediated regulation of 3-methylcholanthrene-induced cytochrome P-450*d* mRNA accumulation in primary rat hepatocyte cultures. *J. Biol. Chem.* **265**:3134–3138 (1990).
10. Pasco, D. S., K. W. Boyum, C. Elbi, C. S. Sin, and J. B. Fagan. Inducer-dependent transcriptional activation of the P4501A2 gene *in vivo* and in isolated hepatocytes. *J. Biol. Chem.* **268**:1053–1057 (1993).
11. Miller, A. G., D. Israel, and J. P. Whitlock, Jr. Biochemical and genetic analysis of variant mouse hepatoma cells defective in the induction of benzo(*a*)pyrene-metabolizing enzyme activity. *J. Biol. Chem.* **258**:3523–3527 (1983).
12. Jones, P. B. C., A. G. Miller, D. I. Israel, D. R. Galeazzi, and J. P. Whitlock, Jr. Biochemical and genetic analysis of variant mouse hepatoma cells which overtranscribe the cytochrome $P_1$-450 gene in response to 2,3,7,8-tetrachlorodibenzo-*p*-dioxin. *J. Biol. Chem.* **259**:12357–12363 (1984).
13. Jones, P. B. C., D. R. Galeazzi, J. M. Fisher, and J. P. Whitlock, Jr. Control of cytochrome $P_1$-450 gene expression by dioxin. *Science (Washington D. C.)* **227**:1499–1502 (1985).
14. Legraverend, C., R. R. Hannah, H. J. Eisen, I. S. Owens, D. W. Nebert, and O. Hankinson. Regulatory gene product of the *Ah* locus: characterization of receptor mutants among mouse hepatoma clones. *J. Biol. Chem.* **257**:6402–6407 (1982).
15. Bradfield, C. A., E. Glover, and A. Poland. Purification and N-terminal amino acid sequence of the *Ah* receptor from the C57BL/6J mouse. *Mol. Pharmacol.* **39**:13–19 (1991).
16. Burbach, K. M., A. Poland, and C. A. Bradfield. Cloning of the Ah-receptor cDNA reveals a distinctive ligand-activated transcription factor. *Proc. Natl. Acad. Sci. USA* **89**:8185–8189 (1992).
17. Wilhelmson, A., S. Cuthill, M. Denis, A. C. Wikstrom, J. A. Gustafsson, and L. Poellinger. The specific DNA binding activity of the dioxin receptor is modulated by the 90 kd heat shock protein. *EMBO J.* **9**:69–76 (1990).
18. Perdew, G. H. Association of the *Ah* receptor with the 90-kDa heat shock protein. *J. Biol. Chem.* **263**:13802–13805 (1988).
19. Nambu, J. R., J. O. Lewis, K. A. Wharton, Jr., and S. T. Crews. The *Drosophila* single-minded gene encodes a helix-loop-helix protein that acts as a master regulator of CNS midline development. *Cell* **67**:1157–1167 (1991).
20. Hoffman, E. C., H. Reyes, F.-F. Chu, F. Sander, L. H. Conley, B. A. Brooks, and O. Hankinson. Cloning of a factor required for activity of the Ah (dioxin) receptor. *Science (Washington D. C.)* **252**:954–958 (1991).
21. Denison, M. S., J. M. Fisher, and J. P. Whitlock, Jr. Protein-DNA interactions at recognition sites for the dioxin-Ah receptor complex. *J. Biol. Chem.* **264**:16478–16482 (1989).
22. Fisher, J. M., L. Wu, M. S. Denison, and J. P. Whitlock, Jr. Organization and function of a dioxin-responsive enhancer. *J. Biol. Chem.* **265**:9676–9681 (1991).
23. Wilson, N. M., M. Christou, C. R. Turner, S. A. Wrighton, and C. R. Jefcoate. Binding and metabolism of benzo[*a*]pyrene and 7,12-dimethylbenz[*a*]anthracene by seven purified forms of cytochrome P-450. *Carcinogenesis (Lond.)* **5**:1475–1483 (1984).
24. Reznikoff, C. A., J. S. Bertram, D. W. Brankow, and C. Heidelberger. Quantitative and qualitative studies of chemical transformation of cloned C3H mouse embryo cells sensitive to postconfluence inhibition of cell division. *Cancer Res.* **33**:3239–3249 (1973).
25. Gehly, E. B., W. E. Fahl, C. R. Jefcoate, and C. Heidelberger. The metabolism of benzo(*a*)pyrene by cytochrome P-450 in transformable and nontransformable C3H mouse fibroblasts. *J. Biol. Chem.* **254**:5041–5048 (1979).
26. Pottenger, L. H., and C. R. Jefcoate. Characterization of a novel cytochrome P450 from the transformable cell line, C3H/10T1/2. *Carcinogenesis (Lond.)* **11**:321–327 (1990).
27. Jones, P. B. C., L. K. Durrin, D. R. Galeazzi, and J. P. Whitlock, Jr. Control of cytochrome $P_1$-450 gene expression: analysis of a dioxin-responsive enhancer system. *Proc. Natl. Acad. Sci. USA* **83**:2802–2806 (1986).
28. Pottenger, L. H., M. Christou, and C. R. Jefcoate. Purification and immunological characterization of a novel cytochrome P450 from C3H/10T1/2 cells. *Arch. Biochem. Biophys.* **286**:488–497 (1991).
29. Otto, S., C. Marcus, C. Pidgeon, and C. Jefcoate. A novel adrenocorticotropin-inducible cytochrome P450 from rat adrenal microsomes catalyzes polycyclic aromatic hydrocarbon metabolism. *Endocrinology* **129**:970–982 (1991).
30. Otto, S., K. K. Bhattacharyya, and C. R. Jefcoate. Polycyclic aromatic hydrocarbon metabolism in rat adrenal, ovary, and testis microsomes is catalyzed by the same novel cytochrome P450 (P450RAP). *Endocrinology* **131**:3067–3076 (1992).
31. Savas, Ü., M. Christou, and C. R. Jefcoate. Mouse endometrium stromal cells express a polycyclic aromatic hydrocarbon-inducible cytochrome P450 that closely resembles the novel P450 in mouse embryo fibroblasts (P450EF). *Carcinogenesis (Lond.)* **14**:2013–2018 (1993).
32. Christou, M., I. M. Keith, X. Shen, M. E. Schroeder, and C. R. Jefcoate. Reversal of cytochrome P-4501A1 and P-450-EF expression in MCA-C3H/10T1/2 cell-derived tumors as compared to cultured cells. *Cancer Res.* **53**:968–976 (1993).
33. Laemmli, U. K. Cleavage of structural proteins during the assembly of the head of bacteriophage T4. *Science (Washington D. C.)* **227**:680–685 (1970).
34. Sambrook, J., E. F. Fritsch, and T. Maniatis. *Molecular Cloning: A Laboratory Manual*, Ed. 2. Cold Spring Harbor Laboratory, Cold Spring Harbor, NY (1989).
35. DuBois, R. N., E. R. Simpson, R. E. Kramer, and M. R. Waterman. Induction of synthesis of cholesterol side chain cleavage cytochrome P-450 by adrenocorticotropin in cultured bovine adrenocortical cells. *J. Biol. Chem.* **256**:7000–7005 (1981).
36. Ivarie, R. D., and P. P. Jones. A rapid sensitive assay for specific protein synthesis in cells and in cell-free translations: use of *Staphylococcus aureus* as an adsorbent for immune complexes. *Anal. Biochem.* **97**:24–35 (1979).
37. Christou, M., P. Stewart, L. H. Pottenger, W. E. Fahl, and C. R. Jefcoate. Differences in the modulation of P450IA1 and epoxide hydratase expression by benz[*a*]anthracene and 2,3,7,8-tetrachlorodibenzo-*p*-dioxin in mouse embryo versus mouse hepatoma-derived cell lines. *Carcinogenesis (Lond.)* **11**:1691–1698 (1990).
38. Kimura, S., F. J. Gonzalez, and D. W. Nebert. Tissue-specific expression of the mouse dioxin-inducible $P_1$450 and $P_3$450 genes: differential transcriptional activation and mRNA stability in liver and extrahepatic tissues. *Mol. Cell. Biol.* **6**:1471–1477 (1986).
39. Poland, A., and E. Glover. Comparison of 2,3,7,8-tetrachlorodibenzo-*p*-dioxin, a potent inducer of aryl hydrocarbon hydroxylase, with 3-methylcholathrene. *Mol. Pharmacol.* **10**:349–359 (1974).
40. Steward, A. R., S. A. Wrighton, D. S. Pasco, J. B. Fagan, D. Li, and P. S. Guzelian. Synthesis and degradation of 3-methylcholanthrene-inducible cytochromes P-450 and their mRNAs in primary monolayer cultures of adult rat hepatocytes. *Arch. Biochem. Biophys.* **39**:494–508 (1985).
41. Knowles, S. E., and F. J. Ballard. Selective control of the degradation of normal and aberrant proteins in Reuber H35 hepatoma cells. *Biochem. J.* **156**:609–617 (1976).
42. Song, B.-J., R. L. Veech, S. S. Park, H. V. Gelboin, and F. J. Gonzalez. Induction of rat hepatic *N*-nitrosodimethylamine demethylase by acetone is due to protein stabilization. *J. Biol. Chem.* **264**:3568–3572 (1989).
43. Voorman, R., and S. D. Aust. Inducers of cytochrome P-450d: influences on microsomal catalytic activities and differential regulation by enzyme stabilization. *Arch. Biochem. Biophys.* **262**:76–84 (1988).
44. Koch, J. A., and D. J. Waxman. P450 phosphorylation in isolated hepatocytes and *in vivo*. *Methods Enzymol.* **206**:305–315 (1991).
45. Israel, D. I., M. G. Estolano, D. R. Galeazzi, and J. P. Whitlock, Jr. Superinduction of cytochrome $P_1$-450 gene transcription by inhibition of protein synthesis in wild-type and variant mouse hepatoma cells. *J. Biol. Chem.* **269**:5648–5653 (1985).
46. Savas, Ü., K. K. Bhattacharyya, M. Christou, D. L. Alexander, and C. R. Jefcoate. Mouse cytochrome P450EF representative of a new 1B subfamily of cytochrome P450s: cloning, sequence determination, and tissue expression. *J. Biol. Chem.*, **269**:14905–14911 (1994).

**Send reprint requests to:** Colin R. Jefcoate, Department of Pharmacology, University of Wisconsin Medical School, 1300 University Avenue, Madison, WI 53706.